arXiv:cond-mat/0608048v1 [cond-mat.mtrl-sci] 2 Aug 2006

Non-collinear magnetism of Cr nanostructures on Fe$_{3ML}$/Cu(001): first–principles and experimental investigations

Samir Lounis[1],* Matthias Reif[2], Phivos Mavropoulos[1], Leif Glaser[2], Peter
H. Dederichs[1], Michael Martins[2], Stefan Blügel[1], and Wilfried Wurth[2]
[1] *Institut für Festkörperforschung, Forschungszentrum Jülich, D-52425 Jülich, Germany*
[2] *Universität Hamburg, Institut für Experimentalphysik,*
Luruper Chaussee 149, D-22761 Hamburg, Germany

A combined experimental, using X-ray Magnetic Circular Dichroism and theoretical investigation, using full-potential Korringa-Kohn-Rostoker (KKR) Green function method, is carried out to study the spin structure of small magnetic Cr adatom–clusters on the surface of 3 monolayers of fcc Fe deposited on Cu(001). The exchange interaction between the different Cr adatoms as well as between the Cr atoms and the Fe atoms is of antiferromagnetic nature and of comparable magnitude, leading due to frustration to complex non-collinear magnetic configurations. The presence of non-collinear magnetic coupling obtained by *ab initio* calculations is confirmed by the experimental results.

The microscopic understanding of the magnetic properties of small transition metal particles has recently attracted a lot of interest. Small clusters show magnetic behavior which is distinctly different from the respective bulk material; for instance, even non-magnetic materials can show magnetism as small clusters [1]. Spin and orbital magnetic moments are usually significantly enhanced when the average coordination number of the atoms is reduced in a cluster [2]. Of particular interest is the tendency of small clusters to favor non-collinear spin structures. In particular, for clusters on surfaces the formation of non-collinear spin structures is observed to relax possible spin frustration which results from a competition between intra-cluster and cluster-substrate interactions. A prototype of such a system are small Cr clusters on a ferromagnetic *fcc* Fe/Cu(001) substrate. The latter one has already challenged experimentalists and theoreticians for several years and is generally accepted to be ferromagnetic (FM) up 4 Fe monolayers[3, 4, 12]. On the other hand Cr atoms tend to couple antiferromagnetically to each other and lead in some cases[5, 6, 7] to non-collinear magnetism.

The aim of this work is to determine the complex magnetism of Cr nanoclusters on Fe/Cu(001) using state-of-the-art theoretical and experimental techniques. Compared to bcc Fe, where adatoms can approach each other at second-neighbor positions at the closest, an fcc(001) Fe substrate allows for a close-packed cluster geometry with first-neighbor positions between adatoms. This enhances the intra-cluster exchange interactions. Furthermore, compared to a Ni substrate, a Fe substrate has a much stronger exchange interaction with the adatoms and ad-clusters. These properties provoke magnetically frustrated states in antiferromagnetic ad-clusters (such as Cr) and make the particular combination of cluster atoms and substrate intriguing.

We first present the *ab-initio* description of this system showing thus the importance of competing intra-cluster and cluster-substrate exchange interaction leading to non-collinear spin structures. The second step consists on depicting the measurements obtained with X-ray Magnetic Circular Dichroism (XMCD) in order to be compared with theory.

TABLE I: Size and angles of magnetic moments in the calculated clusters in the non-collinear configuration. The atoms separated by – have the same magnetic moments and rotation angles.

Cluster	Atom	M (μ_B)	θ (°)	ϕ (°)
Trimer	A, B–C	2.57, 2.92	77, 156	180, 0
Tetra 1	A–D, B–C	2.50, 2.50	111, 111	0, 180
Tetra 2	A, B–D, C	2.85, 2.87, 2.31	172, 176, 13	0, 0, 180
Penta	A, B, C	2.44, 2.47, 2.17	138, 85, 46	0, 180, 180
	D, E	2.48, 2.89	155, 164	0, 0

– *Theory.* Our calculations are based on the Local Density Approximation (LDA) of density functional theory with the parametrization of Vosko *et al.*[8] and use the full-potential non-collinear KKR-Green function method[9, 13]. In the first step the surface Green functions are determined by the screened KKR method [10] for three monolayers of Fe (Fe$_{3ML}$) on Cu(001), using the LDA lattice parameter of Cu (~ 3.51 Å). The obtained magnetic order of Fe is ferromagnetic, with moments for the surface layer of $m_S = 2.66\mu_B$ and the two subsurface layers ($m_{S-1} = 2.09\mu_B$ and $m_{S-2} = 2.18\mu_B$). In the second step we calculate the Green function of the adatoms on the surface, by using the surface Green function as a reference. The resulting cluster of perturbed potentials includes the potentials of the Cr adatoms and the perturbed potentials of several neighboring shells. Angular momenta up to $l_{\max} = 3$ were included in the expansion of the Green functions. We consider all impurities at the unrelaxed hollow position in the first vacuum layer. The orientations assigned to the spin moments of the impurities are always relative to the orientation of the substrate moment, which we take as the global frame [13].

We start with single Cr adatoms, which are antiferromagnetically (AF) coupled to the substrate with an energy difference $\Delta E_{FM-AF} = 564.9$ meV to the ferromagnetic (FM) state, showing the strength of the interaction with Fe. The preference of the AF configuration shows up also in a considerably larger Cr local moment of $3.30\mu_B$ compared to the metastable FM configuration ($2.80\mu_B$). Having established the strong AF coupling of the single adatom, we turn to the adatom dimers. We considered the two adatoms placed as first neighbors with different magnetic configurations. As it turns out the parallel orientation within the dimer, with both atoms antiferromagnetically oriented to the substrate, is the most stable state with Cr moments of $3.02\mu_B$. Surprisingly, we did not find a non-collinear solution which would be expected by the following argument: Both Cr atoms tend to couple AF to the substrate as we have seen for single adatoms, but they also tend to couple AF to each other as expected for elements having a half filled *d*-band and as explained by the Alexander-Anderson model[13, 14]. These competing interactions, should lead to magnetic frustration and to a non-collinear solution. However, when we introduce a rotation of the moments in our *ab-initio* calculations, both impurities relax back to the AF coupling to the substrate even if there is an AF between the dimer atoms. In order to explain this we introduce a Heisenberg model with the exchange parameters calculated from a fit to total energy calculations. We assume a classical spin Hamiltonian of the form $H = -\frac{1}{2}\sum_{i\neq j} J_{ij}\vec{e}_i\vec{e}_j$, where $\vec{e}$ is a unit vector defining the direction of the magnetic moment and i and j indicate the dimer atoms and their first Fe neighbors. Taking into account only first-neighbor interactions and neglecting the rotation of Fe moments, we rewrite the Hamiltonian for the dimer in the form: $H = -J_{\mathrm{Cr-Cr}}\cos(\theta_1+\theta_2) - 4J_{\mathrm{Cr-Fe}}(\cos\theta_1 + \cos\theta_2)$. The angle defining the non-collinear solution is obtained after a minimization of the Heisenberg Hamiltonian: $\cos(\theta_1) = \cos(\theta_2) = -2J_{\mathrm{Cr-Fe}}/J_{\mathrm{Cr-Cr}}$. If $2|J_{\mathrm{Cr-Fe}}| > |J_{\mathrm{Cr-Cr}}|$, the angle is not defined and the non-collinear solution does not exist. This is realized in the present case: $2|J_{\mathrm{Cr-Fe}}| = 2\times 80.8\mathrm{meV} > |J_{\mathrm{Cr-Cr}}| = 77.6$ meV. Note that the Cr-Fe coupling constants are considerably smaller than for the single adatom.

Following the same procedure as for the dimer we first investigated several collinear magnetic configurations for the most compact trimer on the surface, which has the shape of an isosceles rectangular triangle (see Fig. 1(a)). After self-consistency all different collinear configurations converged to the FM solution with drastically reduced moments, *i.e* $0.19\mu_B$ for atom A and $0.42\mu_B$ for both atoms B and C. If we allow the directions of the moments to rotate, the moments strongly increase to “normal” values ($2.57\mu_B$ for atom A and $2.92\mu_B$ for atoms B and C). As seen earlier, the AF interaction within the dimer was not high enough to compete with the adatom-substrate interaction. Addition of a third adatom to the system forces a rotation of the moments. The two second neighboring impurities B and C have a moment tilted down by an angle of 156° and adatom A moment is tilted up with an angle of 77° (Table 1). Thus due to the reduced Fe-Cr coupling the trimer atoms show a nearly antiferromagnetic configuration. The total energy differences between the non-collinear and collinear solution is $\Delta E_{\mathrm{Ncol-FM}} = -360$ meV/adatom.

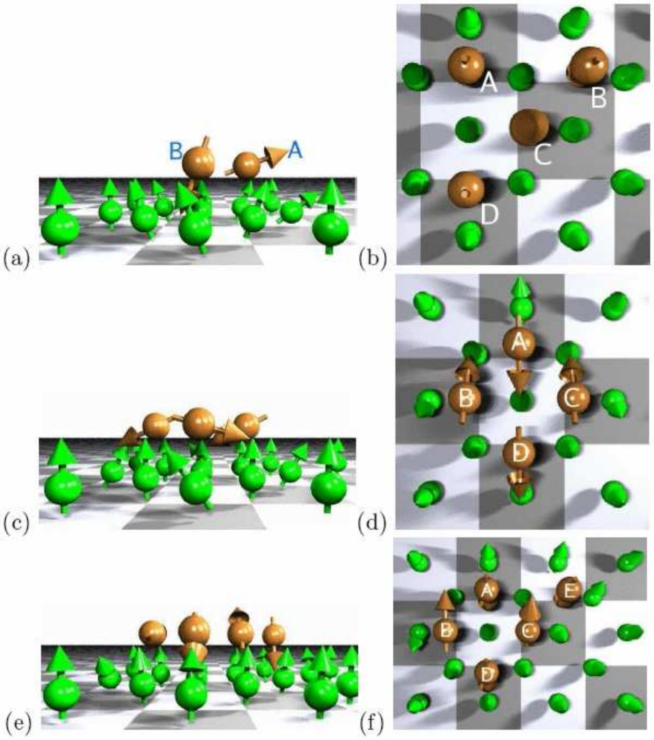

FIG. 1: (Color online) Complex magnetic states of Cr adclusters on Fe_{3ML}/Cu(001) surface: (i) Side view of the trimer is shown in (a) with two Cr atoms pointing down (the second one cannot be seen), (ii) the front view of the T-shape tetramer (tetramer 2) is presented in (b), (iii) both sides of tetramer 1 are shown in (c) and (d), and finally the pentamer is shown in (e) and (f).

We extended our study to bigger clusters, namely tetramers and pentamer. Two types of tetramers were considered: tetramer 1 is the most compact and forms a square (Fig. 1(d)), while tetramer 2 has a T-like shape (Fig. 1(b)). Concerning tetramer 1 (Fig. 1(c) and (d)), two collinear configurations were obtained: the AF solution, where all impurities are coupled antiferromagnetically to the substrate, and a Ferri solution where in each two neighbors within the tetramer are oriented AF to each other. The Ferri state is less stable than the AF as can be seen from the energy difference $\Delta E_{\mathrm{Ferri-AF}} = 543.8$ meV/adatom. The Ferri configuration is characterized by magnetic moments of $-2.45\ \mu_B$ and $2.29\ \mu_B$ whereas in the AF configuration the atoms carry lower moments ($1.94\ \mu_B$). However, the ground state configuration is non-collinear (Fig. 1(c) and (d)) with an energy difference $\Delta E_{\mathrm{AF-Ncol}} = 80$ meV/adatom and a magnetic moment of 2.5 μ_B carried by each impurity. One notices that the first neighboring adatoms are almost AF coupled to each other(the azimuthal angle ϕ is either equal to 0^0 or to 180^0) with all moments rotated by the angle $\theta = 111°$.

For tetramer 2 (see Fig. 1(b)) we obtained several collinear magnetic configurations. The most favorable one is characterized by an AF coupling of the three corner atoms with the substrate. The moment of adatom C, surrounded by the remaining Cr impurities, is then forced to orient FM to the substrate. When we allow for the direction of the magnetic moment to relax, we get a non-collinear solution having a similar picture, energetically close to the collinear one ($\Delta E_{\mathrm{col-Ncol}} =$ 2.3 meV/adatom). Adatom C has now a moment somewhat tilted by 13° ($\mu = 2.31\ \mu_B$) whereas adatom A has a moment tilted in the opposite direction by 172° ($\mu = 2.85\ \mu_B$). Adatoms B and D have a moment of 2.87 μ_B with an angle of 176°. We note that tetramer 1 with a higher number of first neighboring adatom bonds (four instead of three for tetramer 2) is the most stable one ($\Delta E_{\mathrm{tet2-tet1}} = 14.5$ meV/adatom) with the non-collinear solution shown in Fig. 1(c) and (d).

To study the pentamer, we have chosen a structural configuration (Fig. 1(e) and (f)) with the highest number of first neighboring adatom bonds (five). This pentamer consists on a tetramer of type 1 plus an adatom (E) and is characterized by a non-collinear ground state. Let us understand the solution obtained in this case: Tetramer 1 is characterized by a non-collinear almost in-plane magnetic configuration (see Fig. 1(e) and (f)). As we have seen, a single adatom is strongly AF coupled to the substrate. However, when one moves it closer to the tetramer it affects primarily the first neighboring impurity (adatom C) by tilting the magnetic moment from 111° to 46°. Adatom E is also affected by this perturbation and experiences a tilting of its moment from 180° to 164°. As a second effect, the second neighboring adatom, A, is also affected and suffers a moment rotation from 111° to 138°. The AF coupling between first neighboring adatoms is always stable, thus adatom D has also a moment rotated opposite to the magnetization direction of the substrate with an angle of 155° ($\mu = 2.48\ \mu_B$). As adatom B tends to couple AF to its neighboring Cr adatoms, its magnetic moment tilts into the positive direction with an angle of 85°.

– *Experiment.* The magnetic properties of the deposited clusters have been determined experimentally using XMCD. The experiments were performed at the beamline UE56/1- PGM at the BESSY II storage ring in Berlin. The mass selected chromium clusters were generated using a UHV-cluster source [15] and deposited in-situ onto ultrathin Fe layers epitaxially grown on a Cu(100) surface. The iron multilayers were prepared by evaporating iron from a high purity iron sheet onto the clean copper crystal. Subsequently the iron films in the thickness range of ∼3-5 monolayers (ML) were magnetized perpendicular to the surface plane using a small coil. The magnetization of the iron films was monitored by recording Fe 2p XMCD spectra. Before cluster deposition Argon multilayers were frozen onto the iron surface at temperatures below 30K. A layer thickness of 10ML of argon was used to ensure soft landing conditions [16]. After depositing the clusters into the argon buffer layers, the remaining argon was desorbed by flash heating the crystal to ∼80K. Low sample temperatures in the range of 30K and low Cr coverages of 3% of a monolayer (ML) were used to prevent cluster-cluster interaction. The measurements have been carried out at a base pressure $p < 3 \cdot 10^{-10}$mbar. Spectra have been measured from the cluster samples prepared as described above, in a size range of 1 to 13 atoms per cluster. Every step of the preparation has been checked using X-ray Photoelectron Spectroscopy (XPS) and/or X-ray Absorption Spectroscopy (XAS). The absorption signal has been measured using the Total Electron Yield TEY, i.e. the sample current.

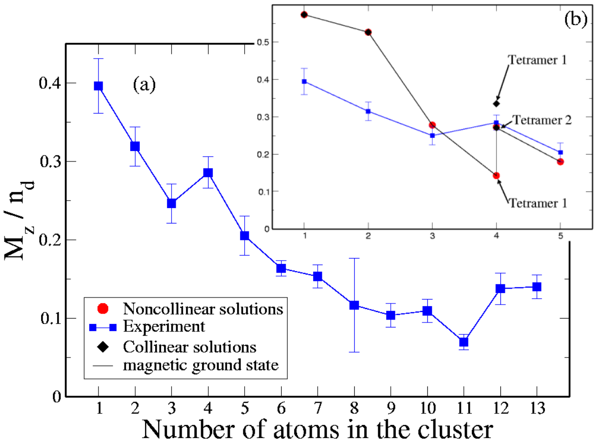

FIG. 2: (Color online) Spin moment per number of d-holes per atom versus cluster size. Fig.a shows the experimental results for cluster-sizes up to 13 adatoms while Fig.b gives the comparison with *ab initio* results for cluster-sizes up to 5 adatoms. Blue squares describe the experimental values, black diamonds show represent collinear configurations, red circles correspond to non-collinear configurations and a black line connects the ratios obtained in the magnetic ground states.

The experimental results for the magnetic moments per d-hole shown in Fig.2 have been determined applying XMCD sum rules [17]. After a standard background treatment, difference and sum spectra are generated by subtraction and addition of the x-ray absorption spectra measured with different photon helicity. A typical exam-

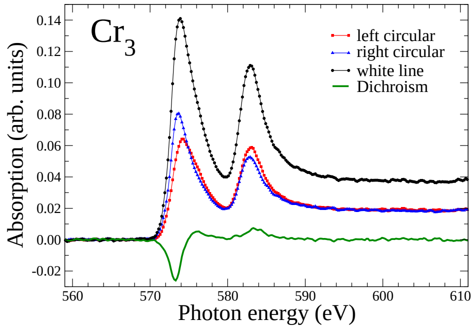

FIG. 3: (Color online) Absorption, difference and sum spectra of a Cr$_3$ cluster.

ple for a Cr$_3$-cluster is shown in Fig.3. For the application of the sum rules, the areas of the 2p$_{3/2}$ and 2p$_{1/2}$ peaks of the difference spectra have been integrated. The 2p$_{3/2}$ peak which shows positive and negative contributions in the difference spectra has been integrated over both contributions. The values for the spin and orbital magnetic moments (not shown) per d-hole have been corrected for a degree of circular polarization of 90%. The contribution of the spin magnetic dipole operator $\langle T_z \rangle$ in the values of the spin moments is presently ignored.

We note that we have applied the XMCD sum rules without empirical corrections which have been proposed for chromium. We are well aware of the fact that due to the problems in the application of the XMCD sum rules for the early transition metals with smaller spin-orbit splitting the absolute values for the spin magnetic moments might be too small by up to a factor of two. However, this will not affect the relative trends seen in the experimental data (Fig. 2.(a)). One notices the strong decrease of S_{eff}/n_d with increasing cluster size which is due to the appearance of antiferromagnetic or non-collinear structures as calculated by theory. The qualitative and quantitative trends observed in the experimental results agree very well with the theoretical results (Fig. 2.(b) for Cr-atoms to Cr-pentamers. Although the theoretical values for Cr-atoms and dimers lie somewhat higher than the experimental values (including error bars) the agreement can still be judged to be very good in view of the remaining experimental uncertainties discussed above. Even details as the increase of spin magnetic moment from trimer to tetramer can be addressed. In order to understand the peak formed for the tetramer we compare in Fig. 2.(b) the ratio between the moment along the z-direction (defined by the magnetization of the substrate) and number of holes per atom obtained by theory for the different geometrical and spin structures. Black circles show the ratio calculated by taking into account the collinear solutions and the red ones show the ratio calculated from the non-collinear solutions. The black line connects the ratio obtained in the magnetic ground states. The non-collinear tetramer 1 has a much lower value than what was seen experimentally whereas the collinear tetramer 1 and tetramer 2 give a better description of the kink seen experimentally. With regards to the small energy difference ($\Delta E = 14.5V$ meV) between the two tetramers we considered, we believe that the experimental value can be understood as resulting from an average of non-collinear tetramers 1, collinear and non-collinear tetramer 2. We believe that this explains why the tetramer ratio value is higher than the one obtained for a trimer. The trimer and the pentamer are clearly well described by the theory and fit to the experimental measurements.

To summarize, the competing exchange interactions in Cr-clusters and with Fe surface atoms affect strongly the complex magnetic structures leading thus to non-collinear magnetism in some cases. This is predicted by DFT calculations and confirmed by XMCD measurements. Considering the complexity of the different clusters and the non-collinear spin structures and the difficult experimental analysis the quantitative agreement between theory and experiment is quite satisfying. A mechanism is proposed to explain the kink observed experimentally for the tetramer in terms of geometrical configuration average. For further corroboration of this result detailed STM investigations with spin-polarization analysis could be envisioned.

This work was financed by the Priority Program "Clusters in Contact with Surfaces" (SPP 1153) of the Deutsche Forschungsgemeinschaft.

---

[*] Electronic address: s.lounis@fz-juelich.de

[1] A. J. Cox, J. G. Louderback and L. A. Bloomfield, Phys. Rev. Lett **71**, 923 (1993).
[2] J. T. Lau, A. Föhlisch, R. Nietubyc, M. Reif and W. Wurth, Phys. Rev. Lett. **89**, 57201 (2002).
[3] J. Thomassen, F. May, B. Feldmann, M. Wuttig, and H. Ibach Phys. Rev. Lett. **69**, 3831 (1992).
[4] T. Asada, S. Blügel, Phys. Rev. Lett. **79**, 507 (1997).
[5] D. Wortmann, S. Heinze, Ph. Kurz, G. Bihlmayer, S. Blügel, Phys. Rev. Lett. **86**, 4132 (2001).
[6] A. Bergman, L. Nordström, A. B. Klautau, S. Frota-Pessôa, and O. Eriksson, Phys. Rev. B **73**, 174434 (2006).
[7] R. Robles, L. Nordström, accepted in Phys. Rev. B (2006).
[8] S. H. Vosko, L. Wilk, and M. Nusair, J. Chem. Phys. **58**, 1200 (1980).
[9] N. Papanikolaou, R. Zeller, and P. H. Dederichs, J. Phys.: Condens. Matter. **14**, 2799 (2002).
[10] K. Wildberger, R. Zeller, and P. H. Dederichs, Phys. Rev. B **55** 10074 (1997) and references therein.
[11] V. S. Stepanyuk, W. Hergert, P. Rennert, B. Nonas, R. Zeller, and P. H. Dederichs, Phys. Rev. B **61**, 2356 (2000).

[12] E. G. Moroni, G. Kresse and J. Hafner, J. Phys.: Condens. Matter **11**, L35 (1999).

[13] S. Lounis, Ph. Mavropoulos, P. H. Dederichs, S. Blügel, Phys. Rev. B **72**, 224437 (2005).

[14] S. Alexander and P. W. Anderson Phys. Rev. **133**, A1594 (1964).

[15] J. T. Lau *et al*, Rev. Sci. Instr. **76**, 063902 (2005).

[16] J. T. Lau, H.-U. Ehrke, A. Achleitner, and W.Wurth, Low Temperature Physics, **29**, 223 (2003).

[17] G. van der Laan, J. Synchrotron Rad., **6**, 694 (1999).